

Shifted Chebyshev reproducing kernel method for flow of an electrically conducting nanofluid over an impermeable stretching cylinder problem

M. Foroutan^a, M.S. Hashemi^b, F. Habibi^b

^aDepartment of Mathematics, Payame Noor University, P.O. Box 19395-3697, Tehran, Iran

^bDepartment of Mathematics, Basic Science Faculty, University of Bonab, Bonab, P.O. Box 55517-61167, Iran

Abstract

In this study a reproducing kernel Hilbert space method with Chebyshev function is proposed for approximating solutions of a nonlinear system of ordinary differential equations under multi-point boundary conditions. Based on reproducing kernel theory, reproducing kernel functions with a polynomial form will be erected in the reproducing kernel spaces spanned by the shifted Chebyshev polynomials. Convergence analysis of the proposed technique is theoretically investigated. This approach is successfully used for solving a system of ordinary differential equations with multi-point boundary conditions arising in flow of an electrically conducting nanofluid over an impermeable stretching cylinder.

Keywords: Reproducing kernel Hilbert space method; shifted Chebyshev polynomials; Convergence analysis; electrically conducting nanofluid

1. Introduction

In this work, we investigate the following nonlinear system of boundary value problems (BVPs) in the reproducing kernel space [1]:

$$\left\{ \begin{array}{l} \Delta_1 \equiv Q(x)f''' + 2\gamma f'' + ff'' - f'^2 - Mf' = 0, \\ \Delta_2 \equiv Q(x)\gamma_R\theta'' + 2\gamma\gamma_R\theta' + P_r(f\theta' - f'\theta - Sf') + Q(x)P_rN_b\theta'\phi' \\ \quad + Q(x)P_rN_t\theta'^2 = 0, \\ \Delta_3 \equiv Q(x)\phi'' + 2\gamma\phi' + L_e(f\phi' - f'\phi - P_e f') + \frac{N_t}{N_b}Q(x)\theta'' + 2\gamma\frac{N_t}{N_b}\theta' = 0, \end{array} \right. \quad (1.1)$$

subject to the boundary conditions

$$\left\{ \begin{array}{l} f(0) = 0, \quad f'(0) = 1 + Af''(0), \\ \theta(0) = 1 - S + B\theta'(0), \quad \phi(0) = 1 - P_e + B_1\phi'(0), \\ f'(\infty) = 0, \quad \theta(\infty) = 0, \quad \phi(\infty) = 0, \end{array} \right. \quad (1.2)$$

Email address: hashemi_math396@yahoo.com, Homepage: <http://rtims.bonabu.ac.ir/~mshashemi/en/> (M.S. Hashemi)

where $Q(x) = 1 + 2\gamma x$, $\gamma_R = 1 + \frac{4}{3}R$, γ is the curvature parameter, M is the magnetic parameter, R is the radiation parameter, N_b is the Brownian motion parameter, N_t is the thermophoresis parameter, P_r is the Prandtl number, L_e is the Lewis number, S is the thermal stratification parameter, P_e is the solutal stratification parameter, A is the velocity slip parameter, B is the thermal slip parameter, and B_1 is the solutal slip parameter. The field of boundary layer flows involving the non-Newtonian fluids is interest of many researchers due to their boundless applications in science and engineering e.g., airfoil design of airplanes, the automobile industry and friction drag of a ship. The governing boundary layer with flow of an electrically conducting nanofluid over an impermeable stretching cylinder equations are reduced into a system of nonlinear ordinary differential equations (ODEs) [2, 3, 4, 5, 6, 7, 8].

It is well-known that ODEs are crucial ingredient of boundary layer flow problems [9, 10, 11, 12]. Systems of ODEs with multi-point boundary conditions erect an interesting class of these problems and play an important role in solving boundary layer flows problems. For nonlinear third and second order multi-point BVPs, there are some reliable approaches to get approximate solutions [13, 14, 15, 16, 17, 18, 19, 20]. Finite difference scheme can easily solve linear BVPs, but it will be cumbersome to investigate nonlinear second and third order with multi-point BVPs using this method. In [21] homotopy analysis method is utilized to approximate the solution of second-order nonlinear BVP. Ahmad in [22] gave the asymptotic form of the solution and utilized this information to develop a series solution. Also, a meshfree method base on the radial basis functions is presented by Kazem et al. [23].

In the current paper, we propose a reliable and powerful method based on reproducing kernel Hilbert space (RKHS) method with orthogonal functions. The RKHS method have been used widely to solve some complicated differential and integral equations arising in science and engineering [24, 25, 26, 27, 28, 29, 30, 31, 32]. In particular, Chebyshev approximations have been considerably used for second (or fourth) ODEs [33, 34, 35, 36]. To the best of our knowledge, there are only few studies which investigate numerical algorithm based upon reproducing kernel Chebyshev functions to solve the nonlinear systems of ODEs with multi-point boundary conditions. We reduce the problem to a set of algebraic equations by expanding the unknown function as orthogonal functions specially constructed on bounded interval, with unknown coefficients. The given operational matrix of derivative along with orthogonal functions are then applied to find the unknown coefficients.

The rest of this paper is organized as follows. In Sect. 2, an overview of shifted Chebyshev polynomials and their relevant properties required henceforward are presented. A shifted Chebyshev reproducing kernel functions are introduced in Sect. 3. In Sect. 4, the collocation scheme to approximate the solution via shifted Chebyshev reproducing kernel basis function is considered. The convergence analysis is discussed in Sect. 5. Finally, Sect. 6, provides some approximate results to show the efficiency and accuracy of using the shifted Chebyshev RKHS method in comparison with of the reported results in [1, 37, 38].

2. shifted Chebyshev polynomials

In this section, a brief summary of shifted Chebyshev polynomial is expressed.

Definition 2.1. *The well-known Chebyshev polynomials of the first kind of degree n are defined on interval $[-1, 1]$ as*

$$C_n(t) = \cos(n\theta), \quad 0 \leq \theta \leq \pi,$$

where $t = \cos(\theta)$. Obviously $C_0(t) = 1$, $C_1(t) = t$, and they satisfy the recurrence relations.

$$C_{n+1}(t) = 2tC_n(t) - C_{n-1}(t), \quad n = 1, 2, \dots \quad (2.3)$$

In order to use these polynomials on the interval $x \in [0, L]$, we define the so called shifted Chebyshev polynomials by introducing the change of variable $t = \frac{2}{L}x - 1$ and this leads to a shifted Chebyshev polynomial $T_n(x)$ of degree in x on $[0, L]$ given by $T_n(x) = C_n(t) = C_n(\frac{2}{L}x - 1)$. Thus we have

$$\begin{aligned} T_0(x) &= 1, \quad T_1(x) = \frac{2}{L}x - 1, \\ T_{n+1}(x) &= 2(\frac{2}{L}x - 1)T_n(x) - T_{n-1}(x), \quad n \geq 1. \end{aligned} \quad (2.4)$$

These polynomials are orthogonal w.r.t. L_w^2 inner product on the $[0, L]$ with the weight function $w(x) = \frac{1}{\sqrt{x(L-x)}}$ and satisfy the orthogonality condition.

$$\int_0^L T_n(x)T_m(x) \frac{1}{\sqrt{x(L-x)}} dx = \frac{\pi}{2} c_n \delta_{nm}, \quad (2.5)$$

where $c_0 = 2$, $c_n = 1, n \geq 1$ and δ_{nm} is the Kronecker delta function. $T_{n+1}(x)$ has exactly $n + 1$ zeros on the interval $[0, L]$. The i th zero x_i is

$$x_i = \frac{L}{2} \left(1 - \cos\left(\frac{(2i+1)\pi}{2n+2}\right) \right), \quad 0 \leq i \leq n.$$

3. Shifted Chebyshev reproducing Kernel function

In this section, some required preliminaries are given to solve the underlying system [28].

Definition 3.1. *Let X be a nonempty set, and \mathcal{H} be a Hilbert space of real-valued functions on some set X with inner product $\langle \cdot, \cdot \rangle_{\mathcal{H}}$. Then, definition $\mathcal{K} : X \times X \rightarrow \mathbb{R}$ is called to be the reproducing kernel function of \mathcal{H} if and only if*

1. $\mathcal{K}(\cdot, y) \in \mathcal{H}$ for all $y \in X$,
2. $\langle f(\cdot), \mathcal{K}(\cdot, y) \rangle_{\mathcal{H}} = f(y)$ for all $y \in X$ and all $f \in \mathcal{H}$.

The second item is well known as the reproducing property.

Assume that

$$u_0(x) = \frac{1}{\sqrt{\pi}}T_0(x), \quad u_n(x) = \sqrt{\frac{2}{\pi}}T_n(x), \quad x \geq 1. \quad (3.6)$$

Now, we have the Christoffel-Darboux formula that shows the explicit reproducing kernel on the finite dimensional space of the shifted Chebyshev polynomials spanned by $\{u_j\}_{j=0}^n$:

Theorem 3.1. ([28]Theorem1.24) For the orthonormal basis functions $\{u_j\}_{j=0}^n$ and

$$\mathcal{K}(x, y) = \langle \mathcal{K}_x, \mathcal{K}_y \rangle_{\mathcal{H}} \equiv \sum_{j=0}^n u_j(x)u_j(y), \quad x, y \in [0, L], \quad (3.7)$$

we have

$$\mathcal{K}(x, y) = \frac{a_n(u_{n+1}(x)u_n(y) - u_n(x)u_{n+1}(y))}{a_{n+1}(x - y)}. \quad (3.8)$$

In this formula, the coefficient of x^n in $u_n(x)$ is presented by $a_n > 0$. Moreover, we have

$$\mathcal{K}(x, x) = \frac{a_n}{a_{n+1}}(u'_{n+1}(x)u_n(x) - u'_n(x)u_{n+1}(x)). \quad (3.9)$$

An easy and straightforward sampling result involving orthonormal basis in the following:

Theorem 3.2. ([29]Theorem1) Let \mathcal{H} be a RKHS of functions defined on a subset Ω with reproducing kernel \mathcal{K} . Assume that there exists a sequence $\{x_n\}_{n=1}^{\infty} \in \Omega$ such that $\{\mathcal{K}(\cdot, x_n)\}_{n=1}^{\infty}$ is an orthogonal basis for H . Then, any $g \in H$ can be expanded as

$$g(x) = \sum_{i=0}^{\infty} g(x_i) \frac{\mathcal{K}(x, x_i)}{\mathcal{K}(x_i, x_i)}, \quad x \in \Omega, \quad (3.10)$$

with convergence absolute and uniform on subset of Ω where the function $x \rightarrow \mathcal{K}(x, x)$ is bounded.

Here, we seek the truncated shifted Chebyshev polynomials with the $(n + 1)$ terms as :

$$\mathcal{P}_n(g)(x) := g_n(x) = \sum_{i=0}^n g(x_i) \frac{\mathcal{K}(x, x_i)}{\mathcal{K}(x_i, x_i)}, \quad x \in [0, L]. \quad (3.11)$$

Corollary 3.1. Let x_n and x_m be the zeros of Chebyshev polynomial $u_{n+1}(x)$ with $x_n \neq x_m$, then

$$\mathcal{K}(x_n, x_m) = \sum_{j=0}^n u_j(x_n)u_j(x_m) = 0.$$

Theorem 3.3. Let \mathcal{H} be a RKHS of shifted Chebyshev polynomials on $[0, L]$ with reproducing kernel \mathcal{K} . Assume that $\{x_i\}_{i=0}^n$ denotes the $n + 1$ simple zero points of u_{n+1} on $(0, L)$. Then, $\{\mathcal{K}(x, x_i)\}_{i=0}^n$ is an orthogonal basis for H .

Proof: Since $\{u_0, u_1, \dots, u_n\}$ is an orthogonal on $[0, L]$ with inner product $\langle u, v \rangle_{\mathcal{H}} = \int_0^L u(x)v(x)w(x)dx$, where $w(x) = \frac{1}{\sqrt{x(L-x)}}$, we have

$$\begin{aligned} \langle \mathcal{K}(x, x_t), \mathcal{K}(x, x_s) \rangle_{\mathcal{H}} &= \left\langle \sum_{i=0}^n u_i(x)u_i(x_t), \sum_{j=0}^n u_j(x)u_j(x_s) \right\rangle_{\mathcal{H}} \\ &= \sum_{i=0}^n u_i(x_t)u_i(x_s) \int_0^L u_i^2(x) \frac{1}{\sqrt{x(L-x)}} dx \\ &= \sum_{i=0}^n u_i(x_t)u_i(x_s). \end{aligned}$$

For $t = s$, we have

$$\langle \mathcal{K}(x, x_t), \mathcal{K}(x, x_s) \rangle_{\mathcal{H}} = \sum_{i=0}^n u_i^2(x_t),$$

and for $t \neq s$, by using corollary 3.1, we have

$$\langle \mathcal{K}(x, x_t), \mathcal{K}(x, x_s) \rangle_{\mathcal{H}} = \sum_{i=0}^n u_i(x_t)u_i(x_s) = 0.$$

Let $\{x_i\}_{i=0}^n$ be the $n+1$ simple zero point of u_{n+1} on $(0, L)$, then by equation (3.8) and (3.9) we have

$$\frac{\mathcal{K}(x, x_j)}{\mathcal{K}(x_j, x_j)} = \frac{u_{n+1}(x)}{u'_{n+1}(x_j)(x - x_j)}, \quad j = 0, 1, 2, \dots, n.$$

Set

$$\varphi_j(x) = \frac{u_{n+1}(x)}{u'_{n+1}(x_j)(x - x_j)}, \quad j = 0, 1, 2, \dots, n, \quad (3.12)$$

then the equation (3.11) changes to

$$g_n(x) = \sum_{j=0}^n g(x_j)\varphi_j(x), \quad j = 0, 1, 2, \dots, n. \quad (3.13)$$

Corollary 3.2. The $\varphi_j(x)$, $j = 0, 1, 2, \dots, n$ are orthogonal w.r.t. $w(x) = \frac{1}{\sqrt{x(L-x)}}$ on $[0, L]$ and satisfy the orthogonality condition

$$\langle \varphi_i(x), \varphi_j(x) \rangle_{\mathcal{H}} = \int_0^L \frac{\varphi_i(x)\varphi_j(x)}{\sqrt{x(L-x)}} dx = \delta_{ij} = \begin{cases} 1, & j = i, \\ 0, & j \neq i. \end{cases}$$

4. Representation of approximate solutions

In order to approximate the Eqs. (1.1)-(1.2) through shifted Chebyshev reproducing function, we first truncate the semi-infinite physical domain $[0, +\infty)$ of the problem into

a finite domain $[0, L]$. Now according to equation (3.13), any function $g(x)$ on $[0, 1]$ can be approximated as

$$g(x) \approx g_n(x) = \sum_{j=0}^n g(x_j) \varphi_j(x) = G^T \psi_n(x), \quad (4.14)$$

where

$$G = [g(x_0), g(x_1), g(x_2), \dots, g(x_n)]^T, \quad (4.15)$$

and

$$\psi_n(x) = [\varphi_0(x), \varphi_1(x), \varphi_2(x), \dots, \varphi_n(x)]^T. \quad (4.16)$$

Note that, the function $\varphi_j(x)$ is satisfy in the following relation

$$\varphi_j(x_i) = \delta_{ij}. \quad (4.17)$$

So, we have $\psi_n(x_j) = e_j$, $j = 0, 1, 2, \dots, n$, where e_j is the $(j+1)^{th}$ column of unit matrix of order $n+1$.

4.1. The operational matrix of derivative

The differentiation of vectors ψ_n in equation (4.16) can be written as

$$\frac{d}{dx} \psi_n = \psi'_n = D \psi_n, \quad (4.18)$$

where D is $(n+1) \times (n+1)$ operational matrix of derivative for shifted Chebyshev reproducing function. Since

$$\left[\frac{d}{dx} \varphi_i \right](x) = \frac{u'_{n+1}(x - x_i) - u_{n+1}(x)}{u'_{n+1}(x_i)(x - x_i)^2}, \quad x \in (0, L), x \neq x_i, 0 \leq i \leq n, \quad (4.19)$$

therefore

$$d_{ij} = \begin{cases} \frac{u'_{n+1}(x_j)}{u'_{n+1}(x_i)(x_j - x_i)}, & i \neq j, \\ \frac{x_i}{2(1 - x_i^2)}, & i = j, \end{cases} \quad (4.20)$$

because, in the case $i = j$, from $u_{n+1}(x_i) = 0$, $i = 0, 1, 2, \dots, n$, we have

$$\lim_{x \rightarrow x_i} \left(\frac{d}{dx} \varphi_i \right) = \lim_{x \rightarrow x_i} \frac{u'_{n+1}(x)(x - x_i) - u_{n+1}(x)}{u'_{n+1}(x_i)(x - x_i)^2} = \frac{u''_{n+1}(x_i)}{2u'_{n+1}(x_i)},$$

and so by Eqs. (2.3), (3.6), and (4.17), we get

$$\lim_{x \rightarrow x_i} \left(\frac{d}{dx} \varphi_i \right) = \frac{x_i}{2(1 - x_i^2)}.$$

4.2. Description of numerical method

In this subsection, we solve the nonlinear BVP (1.1) with multi-boundary condition (1.2). For this purpose, we use equation (4.14) to approximate the function $f(x)$, $\theta(x)$, and $\phi(x)$, then this functions can be expressed as

$$f(x) = F^T \psi_n(x), \quad \theta(x) = E^T \psi_n(x), \quad \phi(x) = H^T \psi_n(x), \quad (4.21)$$

where, F , E , and H are $(n+1) \times 1$ unknown vectors

$$\begin{aligned} F &= [f_0, f_1, f_2, \dots, f_n]^T, \\ E &= [\theta_0, \theta_1, \theta_2, \dots, \theta_n]^T, \\ H &= [\phi_0, \phi_1, \phi_2, \dots, \phi_n]^T. \end{aligned}$$

Equations (4.18) and (4.21) yield

$$f'(x) = F^T D\psi_n(x), \quad f''(x) = F^T D^2\psi_n(x), \quad f'''(x) = F^T D^3\psi_n(x), \quad (4.22)$$

$$\theta'(x) = E^T D\psi_n(x), \quad \theta''(x) = E^T D^2\psi_n(x), \quad (4.23)$$

$$\phi'(x) = H^T D\psi_n(x), \quad \phi''(x) = H^T D^2\psi_n(x). \quad (4.24)$$

Also, using equation (4.14) the function $p(x)$ can be expanded as:

$$Q(x) = \sum_{i=0}^n Q(x_i) \psi_n(x) = Z^T \psi_n(x), \quad (4.25)$$

where

$$Z = [Q(x_0), Q(x_1), \dots, Q(x_n)]^T.$$

Applying equations (4.21)-(4.25) in equations (1.1) and (1.2), we get

$$\left\{ \begin{array}{l} (Z^T \psi_n(x))(F^T D^3 \psi_n(x)) + 2\gamma F^T D^2 \psi_n(x) + (F^T \psi_n(x))(F^T D^2 \psi_n(x)) \\ - (F^T D \psi_n(x))^2 - M F^T D \psi_n(x) = 0, \\ \gamma_R (Z^T \psi_n(x))(E^T D^2 \psi_n(x)) + 2\gamma \gamma_R E^T D \psi_n(x) + P_r [(F^T \psi_n(x))(E^T D \psi_n(x)) \\ - (F^T D \psi_n(x))(E^T \psi_n(x)) - S F^T D \psi_n(x)] + P_r N_b (Z^T \psi_n(x))(E^T D \psi_n(x))(H^T D \psi_n(x)) \\ + P_r N_t (Z^T \psi_n(x))(E^T D \psi_n(x))^2 = 0, \\ (Z^T \psi_n(x))(H^T D^2 \psi_n(x)) + 2\gamma H^T D \psi_n(x) + L_e [(F^T \psi_n(x))(H^T D \psi_n(x)) \\ - (F^T D \psi_n(x))(H^T \psi_n(x)) - P_e F^T \psi_n(x)] + \frac{N_t}{N_b} (Z^T \psi_n(x))(E^T D^2 \psi_n(x)) \\ + 2\gamma \frac{N_t}{N_b} (E^T D \psi_n(x)) = 0, \end{array} \right. \quad (4.26)$$

and

$$\left\{ \begin{array}{l} F^T D \psi_n(0) - A F^T D^2 \psi_n(0) = 1, \quad F^T \psi_n(0) = 0, \\ E^T \psi_n(0) - B E^T D \psi_n(0) = 1 - S, \quad H^T \psi_n(0) - B_1 H^T D \psi_n(0) = 1 - P_e, \\ F^T D \psi_n(L) = 0, \quad E^T \psi_n(L) = 0, \quad H^T \psi_n(L) = 0, \end{array} \right. \quad (4.27)$$

To find the solution in (1.1) we first collocate (4.26) in $x_j = \frac{L}{2}(1 - \cos \frac{(2j+1)\pi}{2n+1})$. So, we get

$$\left\{ \begin{array}{l} (Z^T \psi_n(x_j))(F^T D^3 \psi_n(x_j)) + 2\gamma F^T D^2 \psi_n(x_j) + (F^T \psi_n(x_j))(F^T D^2 \psi_n(x_j)) \\ - (F^T D \psi_n(x_j))^2 - M F^T D \psi_n(x_j) = 0, \quad j = 2, 3, \dots, n-1, \\ \gamma_R (Z^T \psi_n(x_j))(E^T D^2 \psi_n(x_j)) + 2\gamma \gamma_R E^T D \psi_n(x_j) + P_r [(F^T \psi_n(x_j))(E^T D \psi_n(x_j)) \\ - (F^T D \psi_n(x_j))(E^T \psi_n(x_j)) - S F^T D \psi_n(x_j)] + P_r N_b (Z^T \psi_n(x_j))(E^T D \psi_n(x_j))(H^T D \psi_n(x_j)) \\ + P_r N_t (Z^T \psi_n(x_j))(E^T D \psi_n(x_j))^2 = 0, \quad j = 1, 2, \dots, n-1, \\ (Z^T \psi_n(x_j))(H^T D^2 \psi_n(x_j)) + 2\gamma H^T D \psi_n(x_j) + L_e [(F^T \psi_n(x_j))(H^T D \psi_n(x_j)) \\ - (F^T D \psi_n(x_j))(H^T \psi_n(x_j)) - P_e F^T \psi_n(x_j)] + \frac{N_t}{N_b} (Z^T \psi_n(x_j))(E^T D^2 \psi_n(x_j)) \\ + 2\gamma \frac{N_t}{N_b} (E^T D \psi_n(x_j)) = 0, \quad j = 1, 2, \dots, n-1. \end{array} \right. \quad (4.28)$$

Now, by considering equations (4.16) and (4.17), we have

$$\psi_n(x_j) = e_j, \quad j = 1, 2, \dots, n-1, \quad (4.29)$$

where $e_j = [0, 0, \dots, 0, 1, 0, \dots, 0]^T$ is an $(n+1)$ vector, which its j th entry is equal to 1. Finally, by substituting (4.29) into (4.28), we obtain that

$$\left\{ \begin{array}{l} Q(x_j)[F^T D^3]_j + 2\gamma[F^T D^2]_j + F_j[F^T D^2]_j - ([F^T D]_j)^2 - M[F^T D]_j = 0, \quad j = 2, 3, \dots, n-1, \\ \gamma_R Q(x_j)[E^T D^2]_j + 2\gamma \gamma_R [E^T D]_j + P_r (F_j[E^T D]_j - E_j[F^T D]_j - S[F^T D]_j) \\ + P_r N_b Q(x_j)([E^T D]_j)([H^T D]_j) + P_r N_t Q(x_j)([E^T D]_j)^2 = 0, \quad j = 1, 2, \dots, n-1, \\ Q(x_j)[H^T D^2]_j + 2\gamma[H^T D]_j + L_e (F_j[H^T D]_j - [F^T D]_j \\ - P_e [F^T D]_j) \frac{N_t}{N_b} Q(x_j)[E^T D^2]_j + 2\gamma \frac{N_t}{N_b} [E^T D]_j, \quad j = 1, 2, \dots, n-1, \end{array} \right. \quad (4.30)$$

where $[W]_j$ is the j th entry of row vector W .

Equation (4.27) together with equation (4.30), gives a system of algebraic equations, which can be solved to find f_j, θ_j , and ϕ_j , $j = 0, 1, \dots, n$, with using Newton's iterative method. Consequently, the unknown function $f(x)$, $\theta(x)$, and $\phi(x)$ given in equation (4.21) can be calculated.

5. Convergence analysis

In this section, we investigate the convergence analysis of the present method to the approximate solution given by equation (4.14). We assume Π_n denotes the set of polynomials of degree at most n .

Theorem 5.1. [39, p.122] Let $g_n(x) \in \Pi_n$ such that it interpolates $g(x)$ at the $n+1$ distinct points $x_0, \dots, x_n \in [a, b]$. Then for $x \in [a, b]$ there exists $\xi_x \in (\min\{x_i, x\}, \max\{x_i, x\})$ such that

$$g(x) - g_n(x) = \frac{1}{(n+1)!} g^{n+1}(\xi_x) \prod_{i=0}^n (x - x_i). \quad (5.31)$$

Corollary 5.1. Suppose that $g(x) \in C^{n+1}[0, L]$. Let $g_n(x) \in \Pi_n$ be the polynomial that interpolates $g(x)$ at the zero of $u_{n+1}(x)$, the $n+1$ st Chebyshev polynomial. Then

$$\|g - g_n\|_\infty \leq \frac{\sqrt{2}}{\sqrt{\pi} 2^n (n+1)!} \|g^{(n+1)}\|_\infty. \quad (5.32)$$

Proof: By the recursion formula (2.3) and (3.6) the polynomial $u_k(x)$ has the leading coefficient $\sqrt{\frac{2}{\pi}} 2^k$ for $k \geq 1$. Hence

$$u_k(x) = \sqrt{\frac{2}{\pi}} 2^k (x - x_0) \dots (x - x_k).$$

If we choose the $n+1$ interpolation nodes as the zeros of the polynomial $u_{n+1}(x)$ on $[0, L]$, we get

$$\prod_{i=0}^n (x - x_i) = \sqrt{\frac{2}{\pi}} 2^{-n} u_{n+1}(x),$$

and because of $\|u_k\|_\infty = 1$ we obtain

$$\left\| \prod_{i=0}^n (x - x_i) \right\|_\infty = 2^{-n} \sqrt{\frac{2}{\pi}}.$$

Now, from Theorem 5.1, we obtain (5.32).

By using equation (4.14), we have

$$\int_0^L g(x) w(x) dx \approx \int_0^L g_n(x) w(x) dx = \sum_{i=0}^n g(x_i) \int_0^L \varphi_i(x) w(x) dx = \sum_{i=0}^n B_i g(x_i), \quad (5.33)$$

where, the coefficients B_i are given by

$$B_i = \int_0^L \varphi_i(x) w(x) dx, \quad w(x) = \frac{1}{\sqrt{x(L-x)}}. \quad (5.34)$$

Theorem 5.2. [40, Theorem 8.2] If x_k ($k = 0, 1, \dots, n$) are the $n+1$ zeros of $\varphi_n(x)$, and $\varphi_k : k = 0, 1, \dots, n$ is the system of polynomials, φ_k having the exact degree k , orthogonal with respect to $w(x)$ on $[a, b]$, the (5.33) with coefficients (5.34) gives an exact result whenever $g(x)$ is a polynomial of degree $2(n+1)$ or less. Moreover, all the coefficients B_k are positive in this case.

Lemma 5.1. $\|\mathcal{P}_n(g)\|_2 \leq \|g\| (\int_0^L w(x) dx)^{\frac{1}{2}}$.

Proof: Since $\mathcal{P}_n(g)^2$ is a polynomial of degree $\leq 2n < 2(n+1)$, so by using Theorem 5.2, we have

$$\begin{aligned} \|\mathcal{P}_n(g)\|_2^2 &= \int_0^L (\mathcal{P}_n(g))^2 w(x) dx = \sum_{j=0}^n B_j \left(\sum_{i=0}^n g(x_i) \varphi_i(x_j) \right)^2 = \sum_{j=0}^n B_j (g(x_j))^2 \\ &\leq \|g\|^2 \sum_{j=0}^n B_j = \|g\|^2 \int_0^L w(x) dx. \end{aligned} \quad (5.35)$$

Also, we have $\|g\|_2 \leq \|g\| (\int_0^L w(x) dx)^{\frac{1}{2}}$; that is, this same estimate holds for $\|g\|_2$ itself.

Theorem 5.3. Let $\{\varphi_i(x)\}$ be a sequence of orthogonal elements forming a basis for an inner product space $C[0, L]$. Then, for any $g \in C[0, L]$ the truncated series (4.14) converges to $g(x)$, that is

$$\lim_{n \rightarrow \infty} \|g(x) - g_n(x)\| = 0. \quad (5.36)$$

Moreover, if $g \in C^{n+1}[0, L]$, then we have the following inequality:

$$\|g(x) - g_n(x)\|_2 \leq \frac{\sqrt{2}}{2^n(n+1)!} \|g^{n+1}\|_\infty. \quad (5.37)$$

Proof: The equation (5.36) as well as a more general statement of Weierstrass approximation theorem, can be found Atkinson and Han[39]. Now, let $e_n(g) = \|g - g_n^*\|_\infty$, where g_n^* is the best approximation from g_n to $g(x)$ in the L_∞ norm. Hence, by using Lemma 5.1 and by using triangle inequality, we have

$$\begin{aligned} \|g - g_n\|_2 &= \|g - \mathcal{P}_n(g)\|_2 \leq \|g - g_n^*\|_2 + \|\mathcal{P}_n(g - g_n^*)\|_2 \\ &\leq \|g - g_n^*\|_\infty \left(\int_0^L w(x) dx\right)^{\frac{1}{2}} + \|g - g_n^*\|_\infty \left(\int_0^L w(x) dx\right)^{\frac{1}{2}} = 2e_n(g) \left(\int_0^L w(x) dx\right)^{\frac{1}{2}}. \end{aligned}$$

Therefore, it follows from equation (5.32) and $\int_0^L w(x) dx = \int_0^L \frac{1}{\sqrt{x(L-x)}} dx = \pi$ that $\|g - g_n\|_2 \leq \frac{\sqrt{2}}{2^n(n+1)!} \|g^{n+1}\|_\infty$.

Theorem 5.4. Assume that $g(x) \in \mathcal{L}^2[0, L]$ and ε_n is the error between the approximate solution $g_n(x)$ and exact solution $g(x)$. Let $\varepsilon_n^2 = \|g(x) - g_n(x)\|^2$, then, the error sequence $\{\varepsilon_n\}$ is monotone decreasing with regards to the norm of $\mathcal{L}^2[0, L]$ and $\varepsilon_n \rightarrow 0 (n \rightarrow \infty)$.

Proof: The coefficients $g(x_i)$ in equation (3.13) can be determined by

$$\langle g_n, \varphi_i \rangle_{\mathcal{H}} = \left\langle \sum_{j=1}^n g(x_j) \varphi_j, \varphi_i \right\rangle_{\mathcal{H}} = \sum_{j=1}^n g(x_j) \langle \varphi_j, \varphi_i \rangle_{\mathcal{H}} = g(x_i).$$

Therefore

$$\begin{aligned} \varepsilon_n^2 &= \|g(x) - g_n(x)\|^2 = \left\| \sum_{i=n+1}^{\infty} \langle g(x), \varphi_i(x) \rangle_{\mathcal{H}} \varphi_i(x) \right\|^2 = \sum_{i=n+1}^{\infty} \langle g(x), \varphi_i(x) \rangle_{\mathcal{H}}^2, \\ \varepsilon_{n-1}^2 &= \|g(x) - g_{n-1}(x)\|^2 = \left\| \sum_{i=n}^{\infty} \langle g(x), \varphi_i(x) \rangle_{\mathcal{H}} \varphi_i(x) \right\|^2 = \sum_{i=n}^{\infty} \langle g(x), \varphi_i(x) \rangle_{\mathcal{H}}^2, \end{aligned}$$

which implies that $\varepsilon_{n-1} \geq \varepsilon_n$ and shows that the error ε_n is monotone decreasing with regard to $\|\cdot\|_2$. Therefore $\varepsilon_n \rightarrow 0 (n \rightarrow \infty)$.

6. Numerical experiment

In this section, some illustrative examples demonstrate the applicability, efficiency and utility of the proposed technique. Results achieved by the present method are compared

systematically with some of the well-known methods and outperformed in terms of accuracy and generality. The computations associated with the examples were performed using Maple16 on a personal computer.

Let us consider Eqs. (1.1)-(1.2), using the shifted Chebyshev RKHS method. Taking $n = 18$, $L = 8$, and shifted Chebyshev reproducing kernel functions $\varphi_j(x_i)$, $j = 0, 1, \dots, n$ on $[0, 8]$, the numerical solutions $f(x)$, $\theta(x)$ and $\phi(x)$ are obtained by (4.30). Tables 1 and 2 demonstrate the obtained solutions of $f''(x)$ and velocity $f'(x)$ at $x = 0$ with $\gamma = M = 0$, $P_e = B = B_1 = 0.1$ and $L_e = 1.9$ for various values of A and compares the results with homotopy analysis method (HAM), the fourth order Runge-Kutta integration method coupled with the shooting method and closed-form analytical presented in [1, 37, 38], respectively. Table 3 shows the approximate solutions of $f''(x)$ at $x = 0$ with $n = 20$, for different values of A , γ , M and compares the result with the HAM presented in [1]. Table 4 shows the approximate solutions of Nusselt number $-(1 + \frac{4R}{3})\theta'(x)$ at $x = 0$ with $n = 20$, for different values of γ , M , R , P_r , S , N_b and N_t with $P_e = A = B = B_1 = 0.1$, $L_e = 1.9$, $L = 10$ and compares the result with the HAM presented in [1]. The numeric solutions of Sherwood number $-\phi'(x)$ at $x = 0$ with $n = 25$, for different values of P , L_e , A , B , B_1 , γ and M with $R = S = N_b = N_t = 0.1$, $P_r = 1.4$, $L = 12$ and compares the result with the HAM is are demonstrated in Table 5. Good agreement between the result of the shifted Chebyshev RKHS method and other approached are clear.

The effect of magnetic field parameter M on the dimensionless function is exhibited in Figure 1. The dimensionless function $f(x)$, decreased for higher values of the magnetic parameter on $[0, 8]$. The influence of parameter A on $f'(x)$ is plotted in Figure 2 with $L = 8$. This Figure suggests that the $f'(x)$ show decreasing behavior with an increase in A . Figures 3, 4, 5, 6 and Figure 7 display the temperature profiles $\theta(x)$ for the various embedded parameters viz curvature parameter γ , thermal stratification parameter S , Brownian motion parameter N_b , thermophoresis parameter N_t and thermal slip parameter B on interval $[0, 8]$. Also, Figures 8, 9, 10, 11, 12 and Figure 13 display the concentration profiles $\phi(x)$ for the same various parameters.

In order to show the confidence of proposed method, we find the residual errors of the present method by substituting the approximate values of $f(x)$, $\theta(x)$ and $\phi(x)$ in the left hand sides of Δ_1 , Δ_2 and Δ_3 . Fig. 14 demonstrates the residual error w.r.t. the parameters $A = B = B_1 = R = S = P_e = N_b = 0.1$, $\gamma = 0$, $M = 0.2$, $P_r = 1.4$ and $L_e = 1.9$. Maximum errors for the system occur in (a) $x = 0.17$, (b) $x = 0.15$, (c) $x = 0.14$ with values (a) $\|Res(\Delta_1)\|_\infty = 1.82 \times 10^{-07}$, (b) $\|Res(\Delta_2)\|_\infty = 1.02 \times 10^{-05}$ and (c) $\|Res(\Delta_3)\|_\infty = 3.13 \times 10^{-04}$, respectively. In the same manner, Fig. 15 is plotted with parameters $\gamma = B = B_1 = R = S = P_e = N_b = 0.1$, $A = 0$, $M = 0.2$, $P_r = 1.4$ and $L_e = 1.9$. In this case, maximum errors for the system occur in (a) $x = 9.84$, (b) $x = 0.14$, (c) $x = 9.85$ with values (a) $\|Res(\Delta_1)\|_\infty = 3.23 \times 10^{-05}$, (b) $\|Res(\Delta_2)\|_\infty = 1.71 \times 10^{-04}$ and (c) $\|Res(\Delta_3)\|_\infty = 5.60 \times 10^{-04}$, respectively. Finally, Fig. 16 is plotted with parameters $\gamma = A = B = R = S = P_e = 0.1$, $N_b = 1$, $B_1 = 2$, $M = 0.2$, $P_r = 1.4$ and $L_e = 1.9$. In this case, maximum errors for the system occur in (a) $x = 9.84$, (b) $x = 9.85$, (c) $x = 0.14$ with values (a) $\|Res(\Delta_1)\|_\infty = 2.19 \times 10^{-05}$, (b) $\|Res(\Delta_2)\|_\infty = 5.71 \times 10^{-04}$ and (c) $\|Res(\Delta_3)\|_\infty = 1.51 \times 10^{-04}$, respectively.

| A | Anderson [38] | Mahmoud[37] | Hayat et al. [1] | Present |
|------|---------------|-------------|------------------|------------|
| 0.0 | 1.0 | 1.0 | 1.000000 | 1.00000000 |
| 0.1 | 0.8721 | 0.87208 | 0.872082 | 0.87208397 |
| 0.2 | 0.7764 | 0.77637 | 0.776377 | 0.77637890 |
| 0.5 | 0.5912 | 0.59119 | 0.591195 | 0.59119831 |
| 1.0 | 0.4302 | 0.43016 | 0.430159 | 0.43016405 |
| 2.0 | 0.2840 | 0.28398 | 0.283978 | 0.28398629 |
| 5.0 | 0.1448 | 0.14484 | 0.144841 | 0.14485056 |
| 10.0 | 0.0812 | 0.08124 | 0.081242 | 0.08124398 |
| 20.0 | 0.0438 | 0.04378 | 0.043772 | 0.04379099 |

Table 1: Values of $-f''(0)$ for different values of A with $\gamma = M = 0$ and $L = 8$.

| A | Anderson [38] | Mahmoud[37] | Hayat et al. [1] | Present |
|------|---------------|-------------|------------------|-------------|
| 0.0 | 1.0 | 1.0 | 1.00000 | 1.000000000 |
| 0.1 | 0.9128 | 0.91279 | 0.91279 | 0.91279160 |
| 0.2 | 0.8447 | 0.84473 | 0.84473 | 0.84472422 |
| 0.5 | 0.7044 | 0.70440 | 0.70440 | 0.70440084 |
| 1.0 | 0.5698 | 0.56984 | 0.56984 | 0.56983594 |
| 2.0 | 0.4320 | 0.43204 | 0.43204 | 0.43202741 |
| 5.0 | 0.2758 | 0.27579 | 0.27580 | 0.27578010 |
| 10.0 | 0.1876 | 0.18758 | 0.18781 | 0.18768717 |
| 20.0 | 0.1242 | 0.12423 | 0.12456 | 0.12418011 |

Table 2: Results of $f'(0)$ for various values of A with $\gamma = M = 0$ and $L = 8$.

Conclusions

Due to the fact that finding exact solution flow of an electrically conducting nanofluid over an impermeable stretching cylinder problem is usually difficult and in most cases, impossible, we proposed a new computational method for solving them numerically. The shifted Chebyshev reproducing kernel functions as an appropriate class of the basis functions are introduced and used in the implementation of the presented method. In this approach, a truncated series based on shifted Chebyshev reproducing kernel functions with the derivative operational matrixes are used to convert problem (1.1)-(1.2) to a system of nonlinear algebraic equations. The convergence analysis and error estimation of

| γ | M | A | Hayat et al. [1] | Present |
|----------|-----|-----|------------------|------------|
| 0.0 | 0.2 | 0.1 | 0.9511 | 0.95115702 |
| 0.5 | 0.2 | 0.1 | 1.1007 | 1.10077172 |
| 1.0 | 0.2 | 0.1 | 1.2337 | 1.23393640 |
| 0.1 | 0.0 | 0.1 | 0.9021 | 0.90224448 |
| 0.1 | 0.5 | 0.1 | 1.0889 | 1.08895749 |
| 0.1 | 1.0 | 0.1 | 1.2391 | 1.23917550 |
| 0.1 | 0.2 | 0.0 | 1.1352 | 1.13528757 |
| 0.1 | 0.2 | 0.5 | 0.6554 | 0.65544650 |
| 0.1 | 0.2 | 1.0 | 0.4724 | 0.47226763 |
| 0.0 | 0.4 | 0.2 | — | 0.90441894 |
| 0.0 | 0.4 | 0.5 | — | 0.67971087 |
| 0.2 | 0.6 | 0.2 | — | 1.01153444 |
| 0.2 | 0.6 | 0.5 | — | 0.74778935 |

Table 3: Results of $-f''(0)$ for various values of γ , M and A with $L = 10$.

| γ | M | R | P_r | S | N_b | N_t | Hayat et al. [1] | Present |
|----------|-----|-----|-------|-----|-------|-------|------------------|------------|
| 0.0 | 0.2 | 0.1 | 1.4 | 0.1 | 0.1 | 0.1 | 0.9808 | 0.98093232 |
| 0.2 | 0.2 | 0.1 | 1.4 | 0.1 | 0.1 | 0.1 | 1.0343 | 1.03429656 |
| 0.4 | 0.2 | 0.1 | 1.4 | 0.1 | 0.1 | 0.1 | 1.0855 | 1.08592622 |
| 0.1 | 0.4 | 0.1 | 1.4 | 0.1 | 0.1 | 0.1 | 0.9823 | 0.98230681 |
| 0.1 | 0.2 | 0.4 | 1.4 | 0.1 | 0.1 | 0.1 | 1.1603 | 1.16045507 |
| 0.1 | 0.2 | 0.1 | 1.0 | 0.1 | 0.1 | 0.1 | 0.8422 | 0.84241803 |
| 0.1 | 0.2 | 0.1 | 2.0 | 0.1 | 0.1 | 0.1 | 1.2034 | 1.20322728 |
| 0.1 | 0.2 | 0.1 | 1.4 | 0.2 | 0.1 | 0.1 | 0.9732 | 0.97292999 |
| 0.1 | 0.2 | 0.1 | 1.4 | 0.1 | 0.2 | 0.1 | 0.9808 | 0.96867358 |
| 0.1 | 0.2 | 0.1 | 1.4 | 0.1 | 0.1 | 0.2 | 0.9839 | 0.98403543 |
| 0.1 | 0.2 | 0.1 | 1.4 | 0.1 | 0.1 | 0.4 | 0.9392 | 0.93916895 |
| 0.0 | 0.5 | 1.0 | 1.0 | 0.4 | 0.4 | 0.2 | — | 0.82608037 |
| 0.0 | 0.5 | 1.5 | 2.0 | 0.8 | 0.8 | 0.4 | — | 1.02517127 |
| 0.2 | 0.1 | 1.0 | 1.0 | 0.4 | 0.4 | 0.2 | — | 1.01021181 |
| 0.2 | 0.1 | 1.5 | 2.0 | 0.8 | 0.8 | 0.4 | — | 1.15409914 |

Table 4: Results of $-(1 + \frac{4R}{3})\theta'(0)$ for various values of γ , M , R , P_r , S , N_b and N_t with $P_e = A = B = B_1 = 0.1$, $L_e = 1.9$ and $L = 10$.

| γ | P_e | L_e | A | B | B_1 | M | Hayat et al. [1] | Present |
|----------|-------|-------|-----|-----|-------|-----|------------------|------------|
| 0.1 | 0.0 | 1.9 | 0.0 | 0.1 | 0.1 | 0.2 | 0.8176 | 0.81791992 |
| 0.1 | 0.2 | 1.9 | 0.2 | 0.1 | 0.1 | 0.2 | 0.7347 | 0.73498151 |
| 0.1 | 0.4 | 1.5 | 0.2 | 0.1 | 0.1 | 0.2 | 0.5954 | 0.59598138 |
| 0.1 | 0.1 | 2.5 | 0.2 | 0.1 | 0.1 | 0.2 | 1.0010 | 1.00096211 |
| 0.1 | 0.1 | 1.9 | 0.4 | 0.1 | 0.1 | 0.2 | 0.6943 | 6945207558 |
| 0.1 | 0.1 | 1.9 | 0.1 | 0.2 | 0.1 | 0.2 | 0.8100 | 0.81010005 |
| 0.1 | 0.1 | 1.9 | 0.1 | 0.1 | 0.4 | 0.2 | 0.5627 | 0.56262821 |
| 0.0 | 0.0 | 1.0 | 1.0 | 0.2 | 0.1 | 0.4 | — | 0.23638083 |
| 0.0 | 0.2 | 1.5 | 0.5 | 0.2 | 0.2 | 0.4 | — | 0.41138932 |
| 0.2 | 0.4 | 2.0 | 0.5 | 0.2 | 0.1 | 0.4 | — | 0.60913150 |
| 0.2 | 0.6 | 2.5 | 0.2 | 0.4 | 0.1 | 0.6 | — | 0.76862448 |
| 0.2 | 0.8 | 2.9 | 0.2 | 0.4 | 0.4 | 0.6 | — | 0.54426380 |

Table 5: Results of $-\phi'(0)$ for various values of P , L_e , A , B , B_1 , γ and M with $R = S = N_b = N_t = 0.1$, $P_r = 1.4$ and $L = 12$.

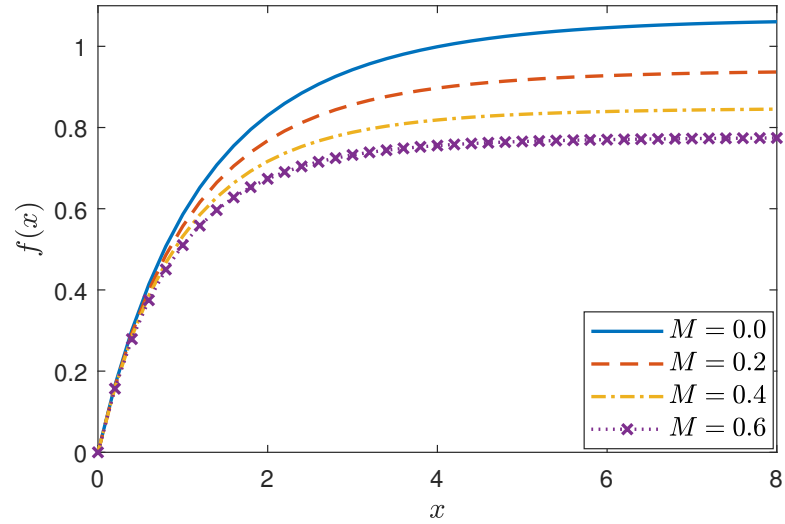


Figure 1: Influence of M on $f(x)$ for values of $\gamma = A = B = B_1 = R = S = P_e = N_b = N_t = 0.1$, $P_r = 1.4$ and $L_e = 1.9$.

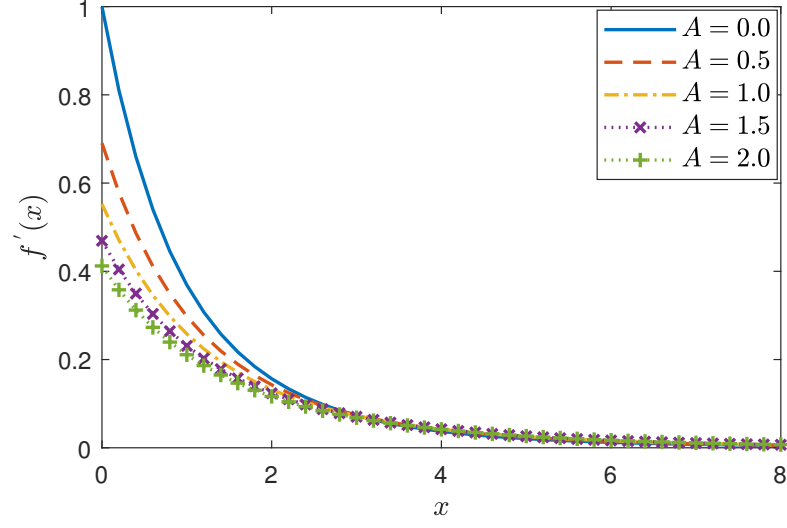


Figure 2: Influence of A on $f'(x)$ for values of $\gamma = B = B_1 = R = S = P_e = N_b = N_t = 0.1$, $M = 0.2$, $P_r = 1.4$ and $L_e = 1.9$.

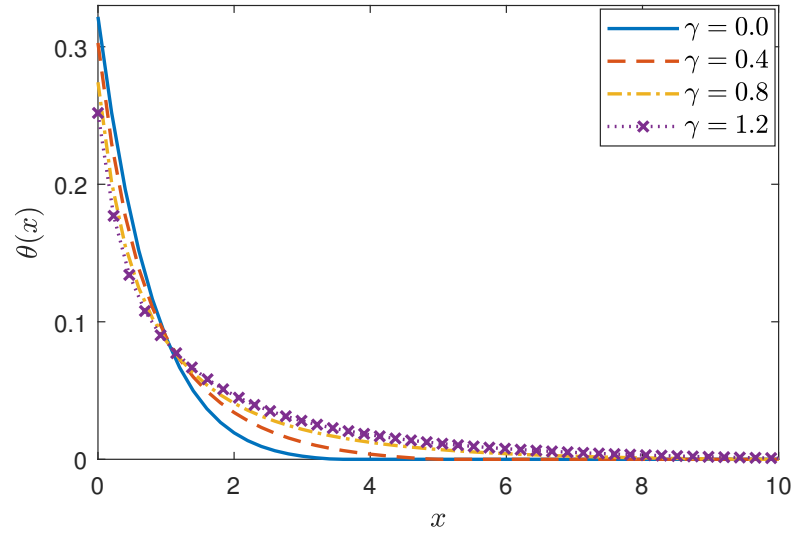


Figure 3: Influence of γ on $\theta(x)$ for values of $A = B_1 = R = S = P_e = N_b = N_t = 0.1$, $B = 1.5$, $M = 0.2$, $P_r = 1.4$ and $L_e = 1.9$.

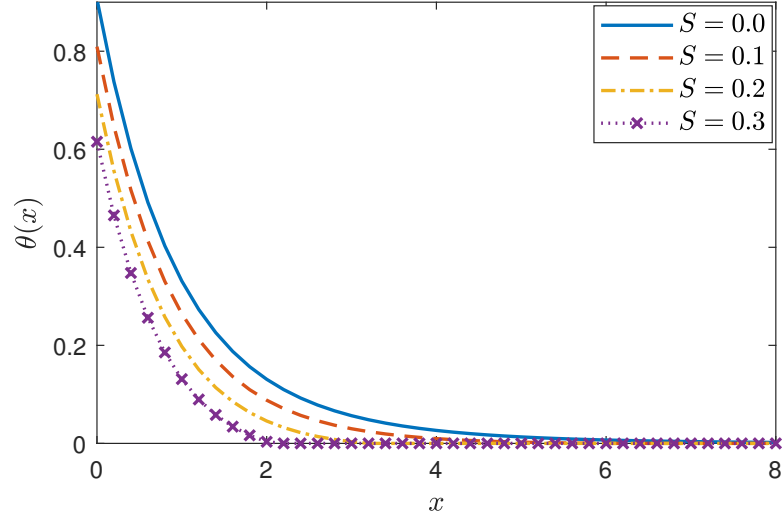


Figure 4: Influence of S on $\theta(x)$ for values of $\gamma = A = B = B_1 = R = P_e = N_b = N_t = 0.1$, $M = 0.2$, $P_r = 1.4$ and $L_e = 1.9$.

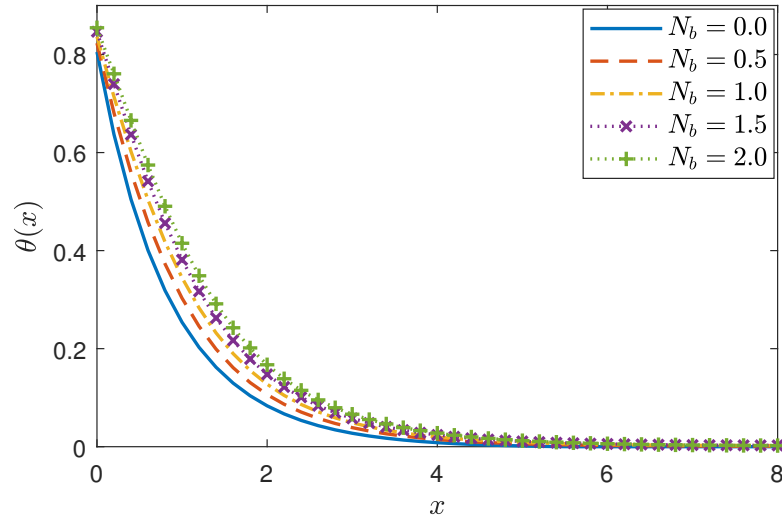


Figure 5: Influence of N_b on $\theta(x)$ for values of $\gamma = A = B = B_1 = R = S = P_e = N_t = 0.1$, $M = 0.2$, $P_r = 1.4$ and $L_e = 1.9$.

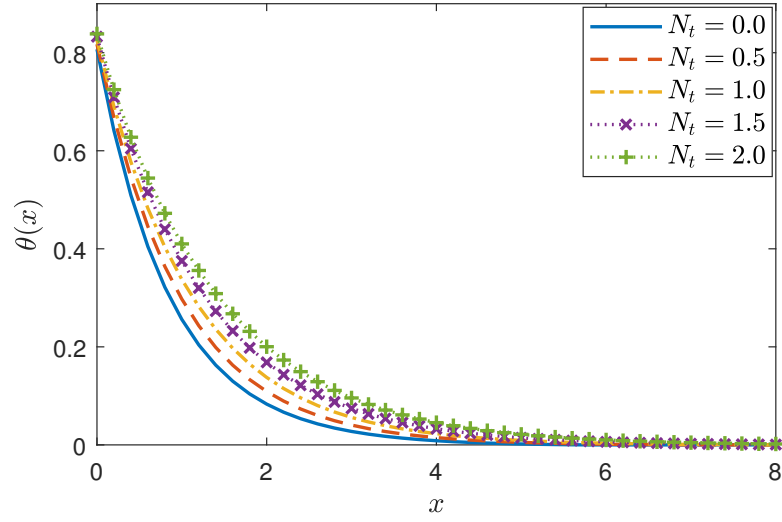


Figure 6: Influence of N_t on $\theta(x)$ for values of $\gamma = A = B = B_1 = R = S = P_e = N_b = 0.1$, $M = 0.2$, $P_r = 1.4$ and $L_e = 1.9$.

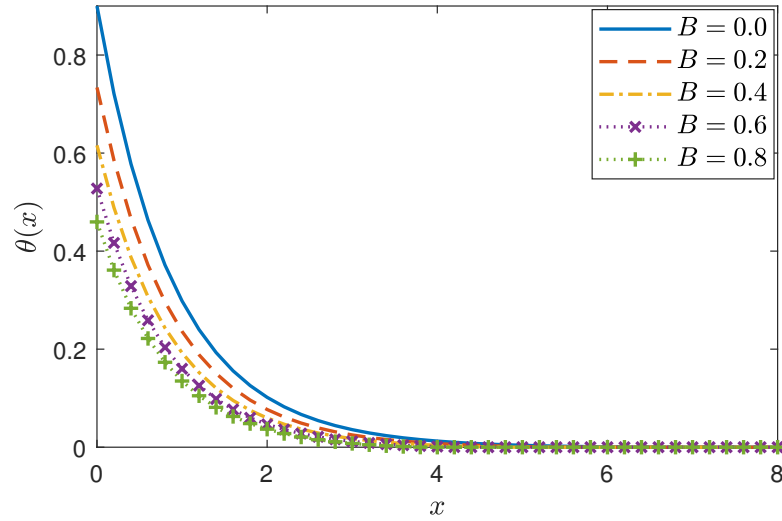


Figure 7: Influence of B on $\theta(x)$ for values of $A = B = B_1 = R = S = P_e = N_b = N_t = 0.1$, $M = 0.2$, $M = 0.2$, $P_r = 1.4$ and $L_e = 1.9$.

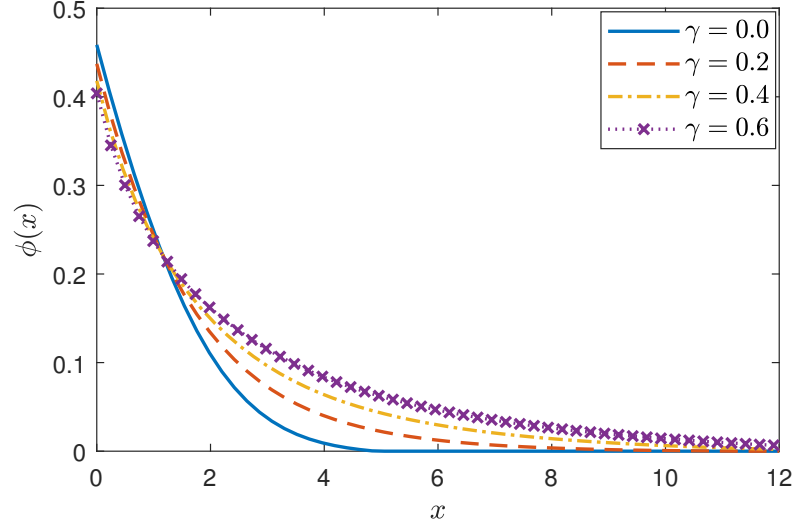


Figure 8: Influence of γ on $\phi(x)$ for values of $A = B = R = S = P_e = N_b = N_t = 0.1$, $B_1 = 1.5$, $M = 0.2$, $P_r = 1.4$ and $L_e = 1.9$.

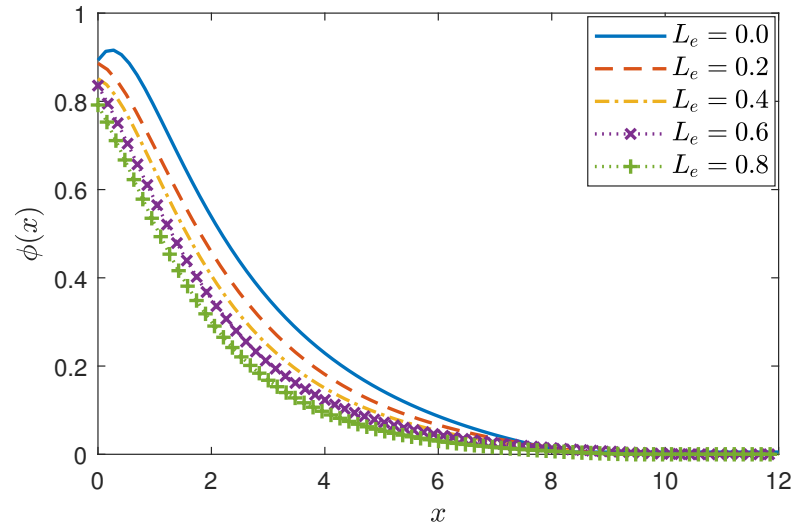


Figure 9: Influence of L_e on $\phi(x)$ for values of $\gamma = A = B = B_1 = R = S = P_e = N_b = N_t = 0.1$, $M = 0.2$ and $P_r = 1.4$.

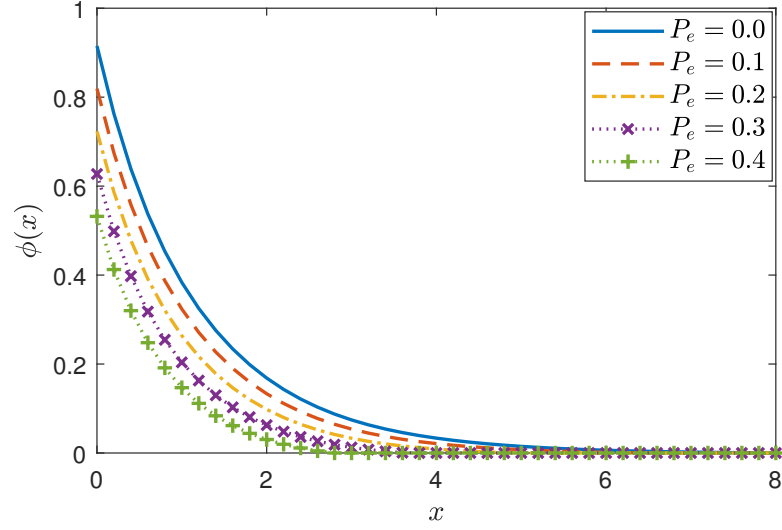


Figure 10: Influence of P_e on $\phi(x)$ for values of $\gamma = A = B = B_1 = R = S = N_b = N_t = 0.1$, $M = 0.2$, $P_r = 1.4$ and $L_e = 1.9$.

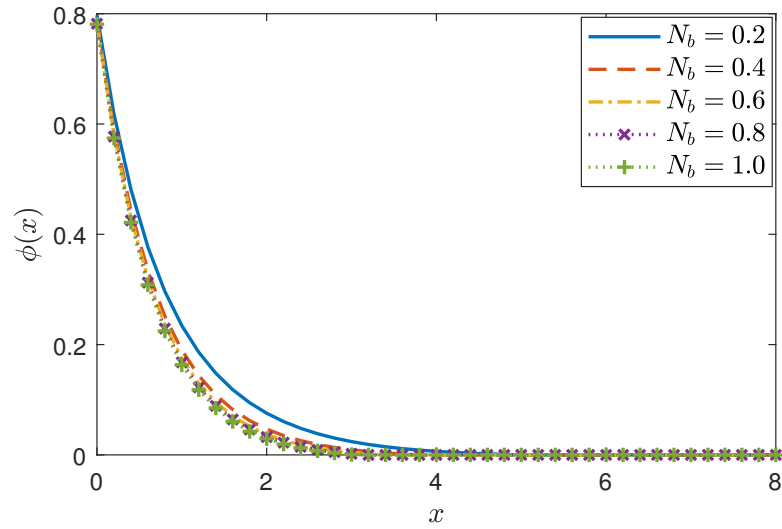


Figure 11: Influence of N_b on $\phi(x)$ for values of $\gamma = A = B = B_1 = R = S = P_e = N_t = 0.1$, $M = 0.2$, $P_r = 1.4$ and $L_e = 1.9$.

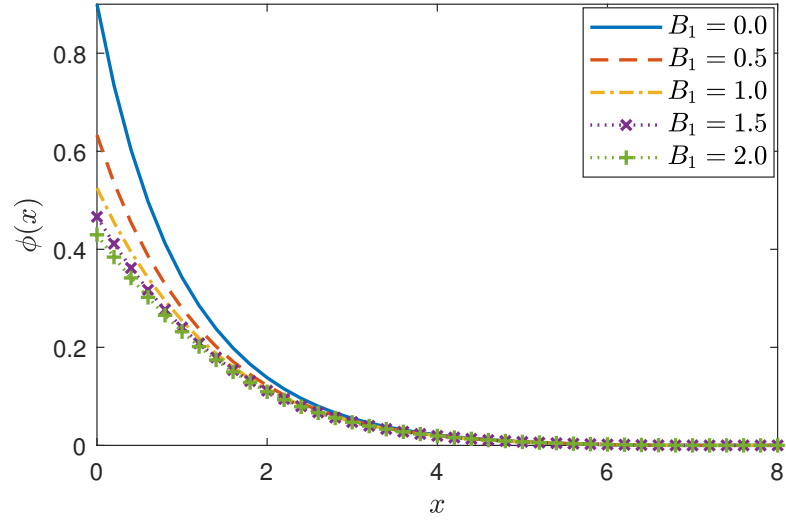


Figure 12: Influence of B_1 on $\phi(x)$ for values of $\gamma = A = B = R = S = P_e = N_b = N_t = 0.1$, $M = 0.2$, $P_r = 1.4$ and $L_e = 1.9$.

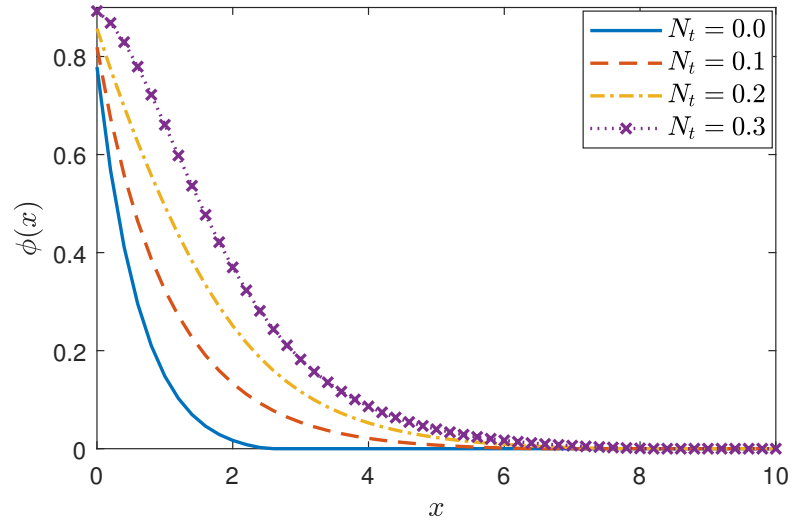


Figure 13: Influence of N_t on $\phi(x)$ for values of $\gamma = A = B = B_1 = R = S = P_e = N_b = 0.1$, $M = 0.2$, $P_r = 1.4$ and $L_e = 1.9$.

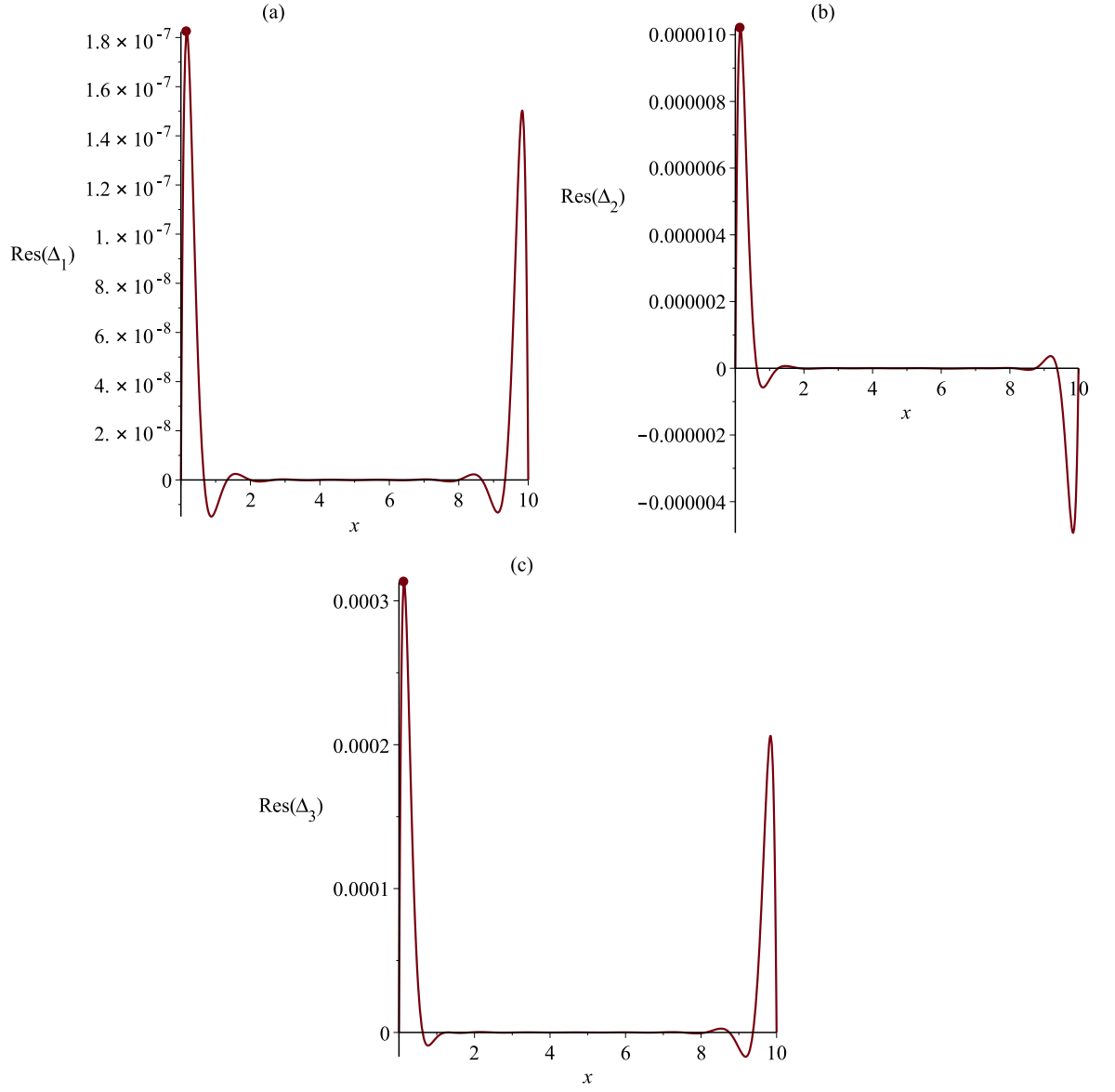


Figure 14: Residual errors with respect to $A = B = B_1 = R = S = P_e = N_b = 0.1$, $\gamma = 0$, $M = 0.2$, $P_r = 1.4$ and $L_e = 1.9$.

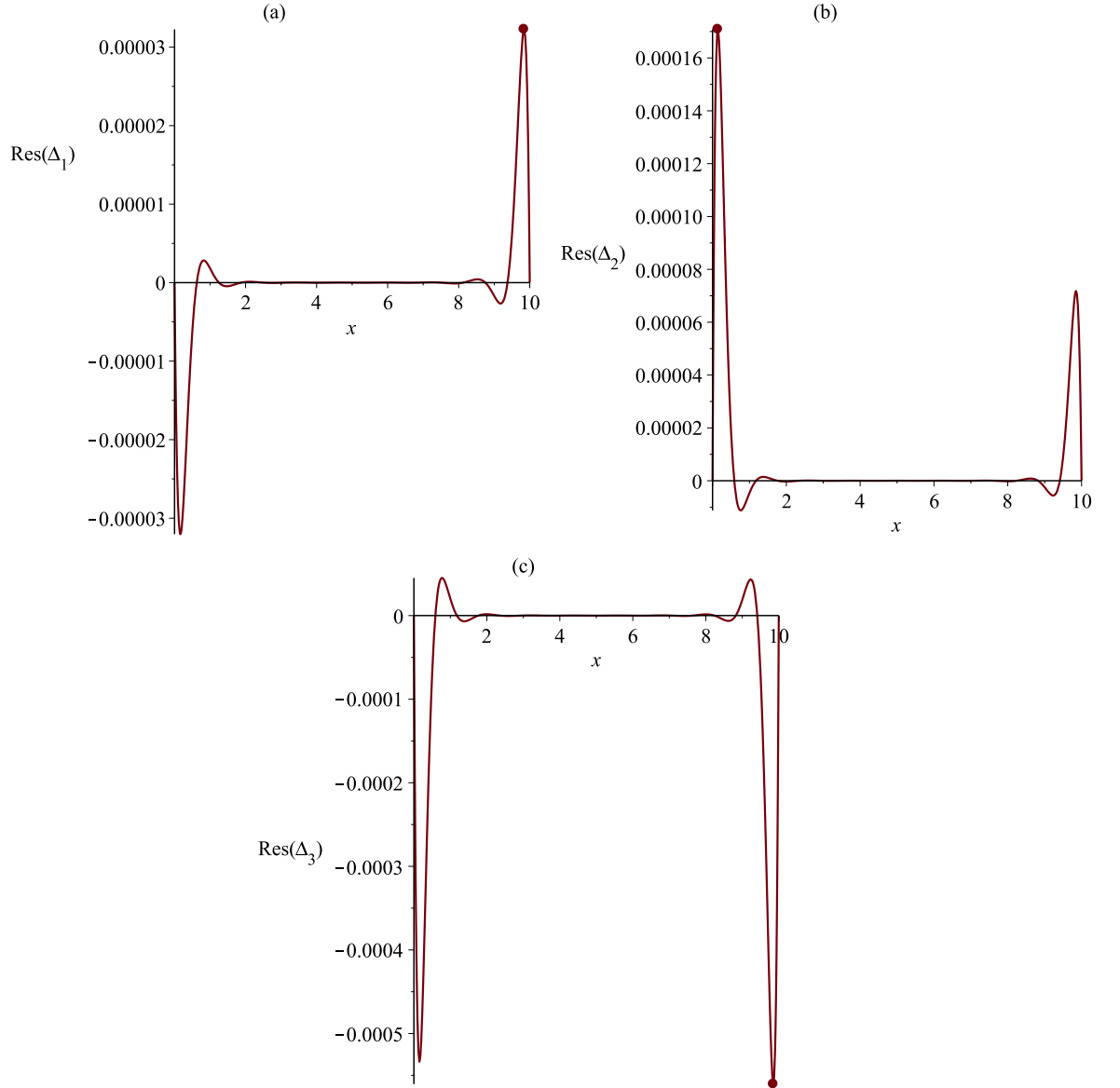


Figure 15: Residual errors with respect to $\gamma = B = B_1 = R = S = P_e = N_b = 0.1$, $A = 0$, $M = 0.2$, $P_r = 1.4$ and $L_e = 1.9$.

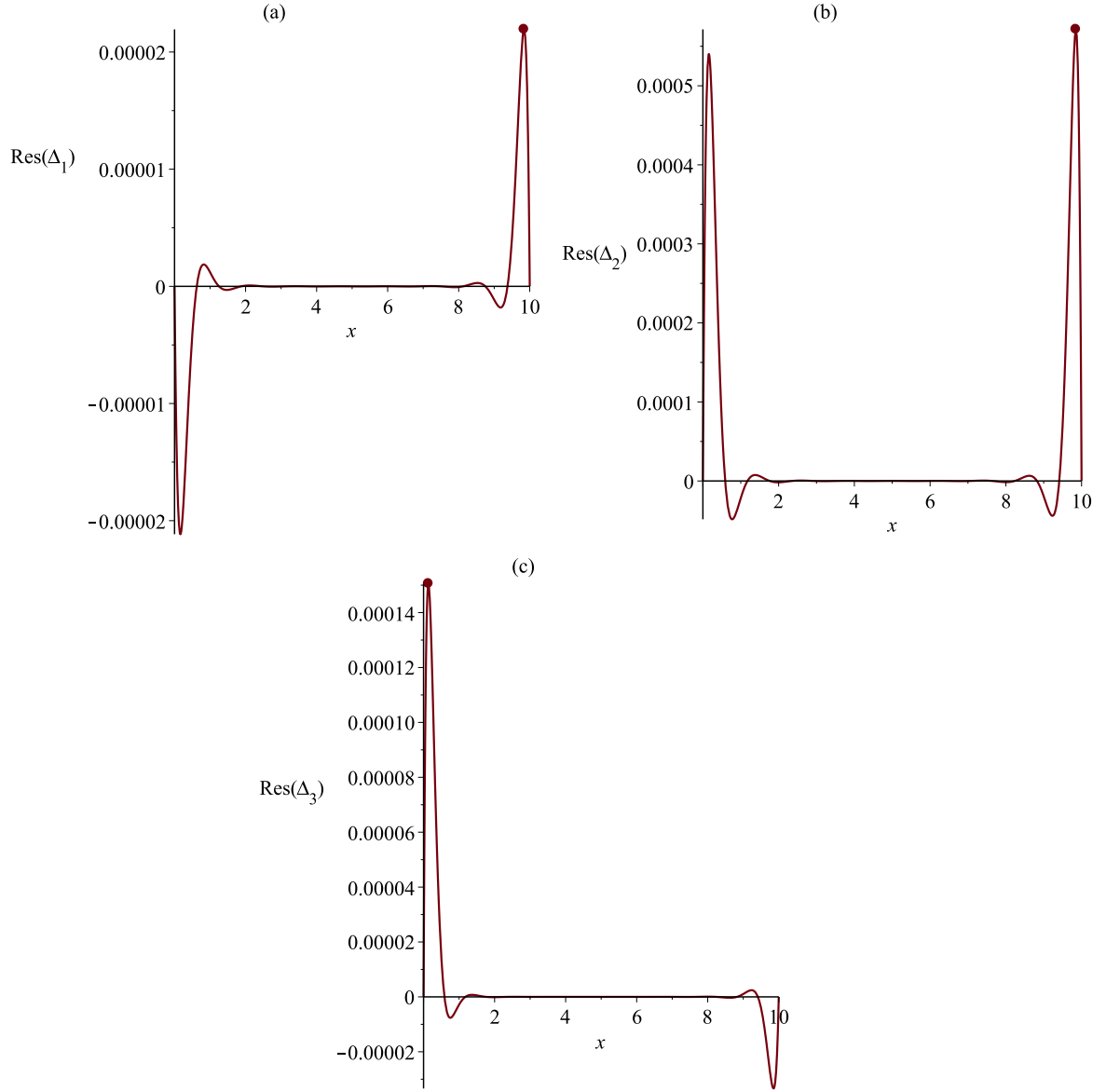


Figure 16: Residual errors with respect to $\gamma = A = B = R = S = P_e = 0.1$, $N_b = 1$, $B_1 = 2$, $M = 0.2$, $P_r = 1.4$ and $L_e = 1.9$.

the approximate solution using the proposed method are investigated. The validity and applicability of the method is demonstrated by solving several numerical examples. The proposed method is a well-performance technique for calculating the best approximate solution of nonlinear multi-point boundary value problems.

- [1] T. Hayat, A. Nasseem, M. I. Khan, M. Farooq, A. Al-Saedi, Magnetohydrodynamic (mhd) flow of nanofluid with double stratification and slip conditions, *Phys Chem Liq* 56 (2) (2018) 189–208.
- [2] M. Inc, A. Akgul, Approximate solutions for mhd squeezing uid ow by a novel method, *Bound Value Probl* 18 (2014) 1–17.
- [3] A. M. Siddiqui, S. Irum, A. R. Ansari, Unsteady squeezing ow of a viscous mhd fluid between parallel plates, *Math Model Anal* 13 (2008) 565–576.
- [4] M. R. Foroutan, A. Ebadian, S. Najafzadeh, Analysis of unsteady stagnation-point flow over a shrinking sheet and solving the equation with rational chebyshev functions, *Math Meth. Appl Sci* 40 (7) (2017) 2610–2622.
- [5] O. Abu Arqub, Numerical solutions for the robin time-fractional partial differential equations of heat and fluid flows based on the reproducing kernel algorithm, *Int J Numer Method H* 28 (2018) 828—856.
- [6] M. S. Hashemi, Constructing a new geometric numerical integration method to the nonlinear heat transfer equations, *Communications in Nonlinear Science and Numerical Simulation* 22 (1-3) (2015) 990–1001.
- [7] M. S. Hashemi, A novel simple algorithm for solving the magneto-hemodynamic flow in a semi-porous channel, *European Journal of Mechanics-B/Fluids* 65 (2017) 359–367.
- [8] M. S. Hashemi, N. Seyfi, M. Bayram, Two reliable methods for solving the forced convection in a porous-saturated duct, *The European Physical Journal Plus* 135 (1) (2020) 29.
- [9] W. Jiang, Z. Chen, Solving a system of linear volterra integral equations using the new reproducing kernel method, *Appl Math Comput* 219 (2013) 10225–10230.
- [10] O. Abu Arqub, The reproducing kernel algorithm for handling differential algebraic systems of ordinary differential equations, *Math Method Appl Sci* 39 (2016) 4549—4562.
- [11] G. Strang, G. Fix, An analysis of the finite element method, Wellesley-Cambridge:Cambridge.
- [12] M. S. Hashemi, A. Akgül, On the mhd boundary layer flow with diffusion and chemical reaction over a porous flat plate with suction/blowing: two reliable methods, *Engineering with Computers* (2019) 1–12.

- [13] M. R. Foroutan, A. Ebadian, A. R., Reproducing kernel method in hilbert spaces for solving the linear and nonlinear four-point boundary value problems, *Int J Comput Math* 95 (10) (2018) 2128–2142.
- [14] M. R. Foroutan, A. R., A. Ebadian, A reproducing kernel hilbert space method for solving the nonlinear three-point boundary value problems, *Int J Numer Model El* 32 (3) (2019) 1–18.
- [15] M. R. Foroutan, A. Ebadian, H. Rahmani Fazli, Generalized jacobi reproducing kernel method in hilbert spaces for solving the black-scholes option pricing problem arising in financial modeling, *Math Model Anal* 23 (4) (2018) 538–553.
- [16] B. Azarnavid, E. Shivanian, K. Parand, S. Nikmanesh, Multiplicity results by shooting reproducing kernel hilbert space method for the catalytic reaction in a flat particle, *Journal of Theoretical and Computational Chemistry* 17 (02) (2018) 1850020.
- [17] L. A. Soltani, E. Shivanian, R. Ezzati, Convection–radiation heat transfer in solar heat exchangers filled with a porous medium: Exact and shooting homotopy analysis solution, *Applied Thermal Engineering* 103 (2016) 537–542.
- [18] R. Ellahi, E. Shivanian, S. Abbasbandy, T. Hayat, Numerical study of magnetohydrodynamics generalized couette flow of eyring-powell fluid with heat transfer and slip condition, *International Journal of Numerical Methods for Heat & Fluid Flow*.
- [19] S. Abbasbandy, H. Roohani Ghehsareh, Solutions of the magnetohydrodynamic flow over a nonlinear stretching sheet and nano boundary layers over stretching surfaces, *International journal for numerical methods in fluids* 70 (10) (2012) 1324–1340.
- [20] S. Abbasbandy, T. Hayat, Solution of the mhd falkner-skan flow by homotopy analysis method, *Communications in Nonlinear Science and Numerical Simulation* 14 (9-10) (2009) 3591–3598.
- [21] T. Hayat, F. Shahzad, M. Ayub, Analytical solution for the steady flow of the third grade fluid in a porous half space, *Appl Math Model* 31 (2007) 2424—2432.
- [22] F. Ahmad, A simple analytical solution for the steady flow of a third grade fluid in a porous half space, *Commun Nonlinear Sci* 14 (2009) 2848—2852.
- [23] S. Kazem, J. A. Rad, K. Parand, S. Abbasbandy, A new method for solving steady flow of a third-grade fluid in a porous half space based on radial basis functions, *Z Naturforsch A* 66a (2011) 591—598.
- [24] S. Abbasbandy, B. Azarnavid, M. S. Alhuthali, A shooting reproducing kernel hilbert space method for multiple solutions of nonlinear boundary value problems, *Journal of Computational and Applied Mathematics* 279 (2015) 293–305.
- [25] P. Bakhtiari, S. Abbasbandy, R. A. Van Gorder, Solving the dym initial value problem in reproducing kernel space, *Numerical Algorithms* 78 (2) (2018) 405–421.

- [26] O. A. Arqub, B. Maayah, Fitted fractional reproducing kernel algorithm for the numerical solutions of abc-fractional volterra integro-differential equations, *Chaos, Solitons & Fractals* 126 (2019) 394–402.
- [27] M. G. Cui, F. Z. Geng, Solving singular two-point boundary problem in reproducing kernel space, *J Comput Appl Math* 205 (1) (2007) 6–15.
- [28] S. Saitoh, Y. Sawano, *Theory of reproducing kernels and applications*, Springer 44.
- [29] A. G. Garcia, Sampling theory and reproducing kernel hilbert spaces, In: *Operator Theory*, D. Alpay Editor, Springer:Basel.
- [30] M. H. Heydari, A new direct method based on the chebyshev cardinal functions for variable-order fractional optimal control problems, *J Franklin I* 355 (2018) 4970–4995.
- [31] A. Akgul, M. S. Hashemi, M. Inc, S. A. Raheem, Constructing two powerful methods to solve the thomas–fermi equation, *Nonlinear Dynamics* 87 (2017) 1435–1444.
- [32] A. Akgül, M. S. Hashemi, et al., Group preserving scheme and reproducing kernel method for the poisson–boltzmann equation for semiconductor devices, *Nonlinear Dynamics* 88 (4) (2017) 2817–2829.
- [33] J. Shen, Efficient spectral-galerkin method. ii. direct solvers of second and fourth-order equations using chebyshev polynomials, *SIAM J Sci Comput* 16 (1995) 74—87.
- [34] J. Shen, T. Tang, L. L. Wang, *Spectral methods: Algorithms, analysis and applications*, Springer-Verlag:NewYork.
- [35] B. Y. Guo, *Spectral methods and their applications*, World Scietific:Singapore.
- [36] C. Canuto, M. Y. Hussaini, A. Quarteroni, T. A. Zang, *Spectral methods in fluid mechanics*, Springer-Verlag:NewYork.
- [37] M. A. Mahmoud, Chemical reaction and variable viscosity effects on flow and mass transfer of a non-newtonian visco-elastic fluid past a stretching surface embedded in a porous medium, *Meccanica* 45 (2010) 835–846.
- [38] H. Andersson, Slip flow past a stretching surface, *Acta Mech* 158 (2002) 121—125.
- [39] K. Atkinson, W. Han, *Theoretical numerical analysis: A functional analysis framework*, Applied Mathematics, vol 39, 3rd edn. Springer.
- [40] J. C. Mason, D. C. Handscomb, *Chebyshev polynomials*, CRC Press.